Proc. of the European Safety and Reliability Conference (ESREL 2026)
Edited by José C. Matos, Paulo B. Lourenço, Michael Beer, Daniel Oliveira,
Edoardo Patelli, Hélder S. Sousa, Rui A. Silva and Monica Santamaria
 Published by Research Publishing, Singapore.
doi: 10.3850/ESREL2026061419_esrel26-p29062-cd

Data-Informed Structural Reliability of Post-Tensioned Concrete Bridges

Ghulam Kibriya

University of Minho, ISISE, ARISE, Department of Civil Engineering, Guimarães, Portugal
E-mail: pg58301@alunos.uminho.pt

Monica Santamaria-Ariza

University of Minho, ISISE, ARISE, Department of Civil Engineering, Guimarães, Portugal
E-mail: msantamaria@civil.uminho.pt

Maria José Morais

University of Minho, ISISE, ARISE, Department of Civil Engineering, Guimarães, Portugal
E-mail: id6741@alunos.uminho.pt

Hélder S. Sousa

University of Minho, ISISE, ARISE, Department of Civil Engineering, Guimarães, Portugal
E-mail: hssousa@civil.uminho.pt

José C. Matos

University of Minho, ISISE, ARISE, Department of Civil Engineering, Guimarães, Portugal
E-mail: jmatos@civil.uminho.pt

Seyedmilad Komarizadehasl

Universitat Politècnica de Catalunya (UPC), Department of Civil and Environmental Engineering, BarcelonaTech, C/ Jordi Girona 1–3, 08034 Barcelona, Spain E-mail: milad.komary@upc.edu

Reliability assessment of existing post-tensioned concrete bridges is often based on finite element models whose support conditions and joint behavior are only approximately known. This can lead to inaccurate stiffness distribution, force redistribution, and collapse resistance in the nonlinear model used for safety evaluation. This article proposes a data-informed workflow for structural reliability assessment that combines numerical modeling and field vibration testing. Operational modal analysis is used to identify modal frequencies and mode characteristics from ambient vibration measurements collected using high quality accelerometers. The identified modal properties are then used to calibrate a finite element model by matching the numerical and measured modal response, with particular attention to support behavior and deck-pier connection stiffness. Reliability is subsequently evaluated for the calibrated bridge using code consistent action models and flexural limit states in critical regions such as midspan sagging and internal support hogging. Uncertainty is represented through random variables for key material properties, loading, prestress, and model uncertainty, while resistance is estimated from nonlinear finite element simulations generated through Latin hypercube sampling. The resulting workflow provides a transparent route from measured bridge dynamics to a calibrated nonlinear OpenSees model and a reliability estimate that is consistent with the observed behavior of the structure.

Keywords: operational modal analysis, bridge model updating, support calibration, structural reliability, post-tensioned concrete bridge, model uncertainty

1. Introduction

Operational modal analysis (OMA) is now a standard route for identifying bridge dynamic properties from ambient vibration measurements without requiring controlled excitation (Peeters and De Roeck 2001; Reynders, Houbrechts, and De Roeck 2012b). For existing bridges, however, the value of OMA extends beyond modal identification itself. It is particularly useful when uncertain support conditions, joint behavior, and local

boundary constraints must be inferred from the measured response rather than prescribed from simplified design assumptions. This is important because a large body of bridge model updating literature identifies support and boundary conditions as some of the most influential and least certain parts of a calibrated finite element (FE) model (Huang et al. 2008; Jaishi and Ren 2007; Cunha et al. 2012; Malveiro et al. 2018; Hester et al. 2019).

That issue becomes critical when dynamic model updating is intended to support safety assessment rather than vibration interpretation alone. If the bridge model used for nonlinear resistance analysis does not reproduce the measured stiffness distribution and support behavior, then the inferred redistribution pattern, support region demand, and collapse resistance may be misrepresented. Monitoring informed reliability updating has been explored in structural health monitoring and Bayesian decision support frameworks (Kamariotis, Chatzi, and Straub 2022, 2023), but most bridge OMA studies stop at linear model updating, condition assessment, or damage identification. In prestressed concrete bridges, this interaction is especially sensitive because deck continuity, support restraint, and prestressing, all contribute to the global response. For that reason, the present study treats model calibration as a prerequisite to reliability assessment rather than as a secondary refinement.

The proposed approach is demonstrated on a roadway bridge in Viana do Castelo, Portugal, through a single continuous workflow from field vibration data to structural reliability. First, OMA is used to extract modal targets from ambient vibration measurements. Second, those targets are used to calibrate a linear FE model while enforcing physically admissible support behavior. Third, the calibrated support parameters are transferred to a nonlinear FE model and propagated through a reliability analysis based on direct nonlinear simulations and model uncertainty factors. The central objective is therefore not to compare two abstract model classes, but to establish a defensible reliability estimate for the actual bridge by grounding the structural model in measured dynamic behavior.

2. Data Informed Reliability Workflow

2.1. *Bridge system and available data*

The bridge is modeled as a post-tensioned deck and pier system with asymmetric end supports and a localized deck-pier interaction zone. The left end behaves as a bearing supported abutment, while the right end provides vertical support without the same bearing idealization. The global in-plane response is therefore sensitive to both translational restraint and local deck pier connection behavior.

The study workflow is summarized as follows. Ambient vibration data from high quality accelerometers were assembled into a multi-setup OMA problem. The resulting modal frequencies and mode shape ordinates were then used as targets for a stagewise FE calibration procedure. The calibrated support parameters were subsequently transferred to a nonlinear FE model implemented in OpenSees, which was used to generate a direct sample of dimensionless peak live load factors under uncertain material, load, and prestress variables. Finally, the sampled peak load response was combined with resistance and load effect model factors to estimate structural reliability.

2.2. *Operational Modal Identification*

The modal targets were extracted from a multi-setup covariance driven stochastic subspace identification analysis carried out with the `pyOMA2` workflow (Pasca and Margoni 2025; Pasca, Sestieri, and D'Ambrogio 2022; Peeters and De Roeck 2001; Reynders, Houbrechts, and De Roeck 2012b; Dohler et al. 2011). The multi-setup datasets were assembled through the Pre-Global Estimation Re-scaling (PreGER) procedure, and modal identification was then performed with multi-setup stochastic subspace identification (SSI-MS). Three ambient vibration datasets were assembled from the field campaign, with two common reference channels retained across setups and roving channels used to extend the observable bridge geometry. In the processed run used for calibration, the records were resampled to $200\,\mathrm{Hz}$, high pass filtered at $0.1\,\mathrm{Hz}$, low pass filtered at $40\,\mathrm{Hz}$, and truncated to the first $600\,\mathrm{s}$ of each

setup before multi-setup assembly. The covariance driven SSI analysis used 120 block rows and a maximum model order of 120, after which stable poles were clustered over the 0.2 Hz to 40 Hz band using a 0.05 Hz frequency tolerance.

This procedure follows the standard OMA logic of extracting stabilization columns from a parametric pole cloud and then selecting representative poles from stable clusters (Magalhaes, Cunha, and Caetano 2009; Reynders, Houbrechts, and De Roeck 2012a; Brownjohn et al. 2010). Figure 1 shows the identification diagnostics. Since the retained calibration modes lie below 10 Hz, the figure is restricted to that low frequency range, where the stable pole columns relevant to the bridge are most clearly visible.

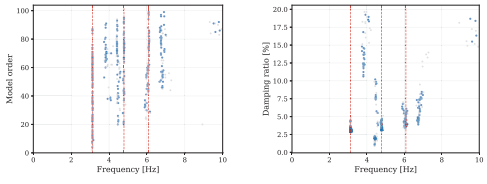

(a) (b)

Fig. 1. Operational modal identification diagnostics from the multi-setup covariance driven SSI run, restricted to the 0 Hz to 10 Hz band that contains the calibration modes: (a) stabilization diagram and (b) damping frequency distribution of the same pole set.

After stable poles were identified, representative modal vectors were phase aligned and reduced to the sensor space used in the calibration model. The first three modes were retained because they are the dominant global in-plane modes and carry the strongest information on support condition sensitivity in the present bridge model. The identified targets are listed in Table 1.

Table 1. Identified modal targets used for FE calibration.

Mode	Frequency [Hz]	Damping ratio [-]
1	3.122914	0.0282
2	4.779113	0.0452
3	6.061945	0.0440

2.3. *Finite Element calibration*

The FE calibration was formulated as a stage-wise updating problem rather than a single unrestricted optimization. This choice follows the bridge model updating literature, where progressive updating is often used to avoid compensating one modeling error with another and to maintain parameter identifiability (Cunha et al. 2012; Malveiro et al. 2018; Hester et al. 2019). In the present bridge, that issue is especially relevant at the supports. Rotational restraint at the abutments was therefore fixed near zero throughout the calibration because the actual support details do not justify significant end moment restraint.

Mode pairing between measured and numerical modes was performed automatically via a Hungarian assignment using a combined cost comprising relative frequency mismatch and a modal assurance criterion (MAC) penalty. Once paired, the residual vector for the optimizer was assembled from weighted frequency residuals, MAC residuals, signed mode shape differences in sensor space, soft penalties for poor mode pairing, and prior regularization on the active parameter set. In compact form,

$$\mathbf{r}(\boldsymbol{\theta}) = \Big[w_f r_f,\ w_{\mathrm{MAC}}(1-\mathrm{MAC}),\ w_\phi \Delta\boldsymbol{\phi},\ \mathbf{r}_{\mathrm{pair}},\ \mathbf{r}_{\mathrm{prior}} \Big] \tag{1}$$

where $\boldsymbol{\theta}$ is the vector of calibration parameters, r_f is the relative frequency residual, MAC is the modal assurance criterion between paired measured and numerical mode shapes, $\Delta\boldsymbol{\phi}$ is the signed mode shape residual in sensor space, and w_f, w_{MAC}, and w_ϕ are the corresponding weights. The pairing term $\mathbf{r}_{\mathrm{pair}}$ penalizes unacceptable frequency mismatch and low MAC, and the prior term $\mathbf{r}_{\mathrm{prior}}$ regularizes the active parameters around physically reasonable initial values. Similar residual based formulations are widely used in bridge model updating to combine frequency, shape, and regularization terms in a single optimization problem (Jaishi and Ren 2007; Cunha et al. 2012).

The optimization itself was staged. In Stage 1, the active variables were the left and right

abutment vertical stiffnesses and the rotational stiffness of the pier-deck joint, and the residual vector emphasized frequency matching. In Stage 2, the vertical stiffness of the pier deck joint was released, and the full residual vector, including MAC and shape terms, was activated. Each stage used a global differential evolution search followed by local least squares refinement, with the final mode pairing frozen before the local step. This procedure proved more stable than releasing all support parameters from the beginning.

2.4. *Nonlinear Model and Reliability Formulation*

The calibrated support model was transferred to a nonlinear finite element model implemented in OpenSees (McKenna 2011; McKenna, Scott, and Fenves 2010). Prestress was represented through truss based tendon elements, and the deck and piers were modeled with nonlinear sections. Concrete was modeled with the ASDConcrete1D uniaxial material, which provides a plastic damage formulation with tensile and compressive softening and optional regularization features (OpenSees Documentation 2026). Reinforcing and prestressing steel were represented with explicit strain limits consistent with the section level limit state checks adopted in the nonlinear analysis. The live load response was traced by displacement control, and the structural resistance variable was taken as the dimensionless peak converged live load factor from each analysis rather than the terminal factor at the end of the loading path. This distinction is important because some analyses exhibited post peak softening and redistribution.

The random variables adopted in the reliability analysis are summarized in Table 2. These quantities were treated directly as mean values with assigned coefficients of variation, and Latin hypercube sampling was used to generate 200 nonlinear FE realizations for the calibrated bridge model (McKay, Beckman, and Conover 1979). Reliability was then evaluated from the sampled peak load factor response of the nonlinear model. A normal distribution was fitted to the dimensionless peak live load factor, denoted LF, and reliability was evaluated with the limit state function

$$g = \theta_R \cdot \mathrm{LF} - \theta_S, \tag{2}$$

where LF is the dimensionless peak live load factor, θ_R is the resistance model uncertainty factor, and θ_S is the load effect model uncertainty factor. This multiplicative formulation follows the JCSS treatment of model uncertainties (Joint Committee on Structural Safety 2023; Melchers and Beck 2017). For the primary reliability estimates reported below, the JCSS values for frame moment load effects and concrete bending resistance were adopted: $\theta_S \sim \mathrm{LN}(\mu = 1.0, \mathrm{CoV} = 0.10)$ and $\theta_R \sim \mathrm{LN}(\mu = 1.2, \mathrm{CoV} = 0.15)$.

3. Results

The results are presented in the same order as the workflow itself. The section first summarizes the modal identification and calibration outcome, then describes the calibrated nominal nonlinear response, and finally reports the sampled reliability response of the calibrated bridge.

3.1. *Modal Identification and Calibration Outcome*

The OMA and FE updating stages produced a consistent low order dynamic description of the bridge. The calibrated support model reproduced the first three retained modes with a mean absolute frequency error of 3.55%, a maximum absolute frequency error of 5.50%, and a mean MAC of 0.959. Figure 2 summarizes the frequency agreement and MAC values. Figure 3 compares the identified OMA modal ordinates with the matched FE deflection shapes; the dashed gray lines indicate the undeformed FE geometry, the blue lines the FE mode shapes, and the red points the OMA ordinates. In practical terms, this means that the updated model reproduced both the modal stiffness level and the dominant deflected shape characteristics of the measured bridge sufficiently well to justify its use as the starting point for nonlinear assessment.

The value of the calibration is not only numerical. The updated support set is mechanically interpretable: abutment rotations remain essentially free, vertical abutment stiffnesses remain

Table 2. Random variables used in the calibrated reliability analysis.

Variable	Mean	CoV	Distribution
Reinforcing steel elastic modulus E_s [GPa]	202.0	0.05	Normal
Reinforcing steel yield strength f_y [MPa]	480.0	0.10	Normal
Prestressing steel elastic modulus E_p [GPa]	202.0	0.05	Normal
Prestressing steel strength f_{py} [MPa]	1679.9	0.023	Normal
Pier concrete elastic modulus $E_{cm,p}$ [GPa]	32.78	0.08	Normal
Pier mean compressive strength $f_{cm,p}$ [MPa]	37.8	0.047	Normal
Pier tensile strength $f_{ctm,p}$ [MPa]	3.38	0.20	Normal
Deck concrete elastic modulus $E_{cm,d}$ [GPa]	34.12	0.08	Normal
Deck mean compressive strength $f_{cm,d}$ [MPa]	43.2	0.047	Normal
Deck tensile strength $f_{ctm,d}$ [MPa]	3.69	0.20	Normal
Concrete density ρ_c [kg/m^3]	2400	0.05	Normal
Midspan point live load P_L [kN]	500.0	0.15	Gumbel
Distributed live load q_L [kN/m]	79.5	0.15	Gumbel
Initial prestress σ_{p0} [MPa]	1030.0	0.06	Normal
Superimposed dead load q_D [kN/m]	23.415	0.15	Normal

finite rather than being idealized as perfectly rigid, and pier-deck joint stiffnesses are identified directly from the measured bridge response. The calibrated values are listed in Table 3. This is the essential link between the OMA stage and the nonlinear stage. The dynamic calibration is not presented here as an end in itself; it is the mechanism by which the nonlinear model inherits physically admissible support behavior.

Table 3. Support parameters transferred from modal calibration to the nonlinear bridge model.

Parameter	Value
$k_{x,\text{left}}$	1000.0
$k_{y,\text{left}}$	1.003×10^6
$k_{r,\text{left}}$	0.001
$k_{x,\text{right}}$	1000.0
$k_{y,\text{right}}$	9.937×10^5
$k_{r,\text{right}}$	0.001
$k_{x,\text{joint}}$	1093.3
$k_{y,\text{joint}}$	9.917×10^7
$k_{r,\text{joint}}$	1323.3

3.2. *Calibrated Nominal Nonlinear Response*

The nominal calibrated nonlinear analysis reached a dimensionless peak load factor of 2.833 and

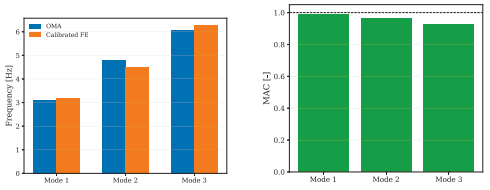

(a) (b)

Fig. 2. Modal calibration summary for the final support updated linear FE model: (a) identified and calibrated modal frequencies and (b) MAC values for the matched modes.

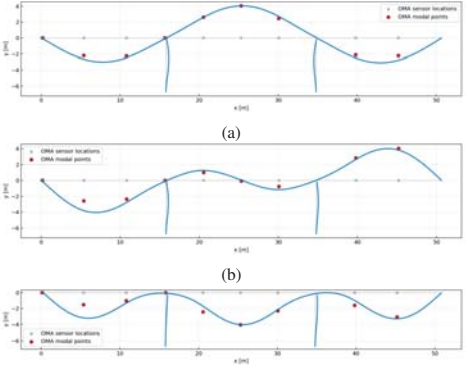

(a)

(b)

(c)

Fig. 3. Comparison between the matched FE deflected shapes and the identified OMA modal points for the first three retained modes: (a) Mode 1, (b) Mode 2, and (c) Mode 3.

terminated by *ultimate strain*, indicating that the traced response reached the imposed section level failure criterion rather than stopping through numerical breakdown. Figure 4 summarizes the nominal nonlinear response (black curve) together with the calibrated response ensemble (gray curves). The nominal trace sits within the broader cloud of realizations and remains representative of the support region controlled behavior identified in the nonlinear model.

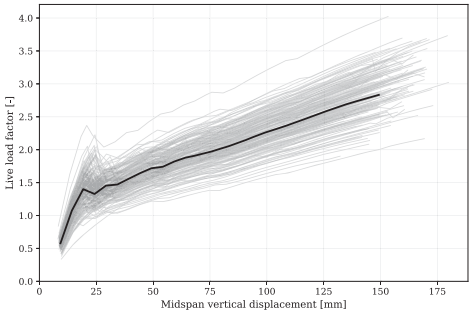

Fig. 4. Live load factor versus midspan vertical displacement for the calibrated nonlinear OpenSees model.

This nominal response is important because it shows that the calibrated model can be carried to a physically defined failure state while remaining consistent with the broader family of nonlinear calibrated realizations. The nominal trace, therefore, provides a useful reference response for interpreting the reliability sample discussed in the next subsection.

3.3. *Calibrated Reliability Response Sample*

The reliability study used the 200 nonlinear FE realizations directly as the resistance sample. The resulting dimensionless peak load factor sample had a mean of 2.872, a standard deviation of 0.385, a median of 2.870, a 5th percentile of 2.214, and a 95th percentile of 3.497. All 200 realizations in the training sample reached *ultimate strain*, and no FE realization fell below the failure threshold of $\mathrm{LF} = 1.0$. Figure 5 shows the fitted normal distribution (red curve) together with the sample histogram, the failure threshold (dotted vertical line), and the nominal peak load factor (dashed vertical line).

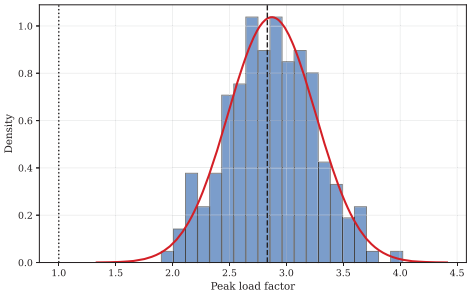

Fig. 5. Histogram of the 200 FE peak load factor realizations for the calibrated bridge model with fitted normal density.

When the response sample was combined with the JCSS model uncertainty factors, the resulting failure probability estimate was 1.00×10^{-6}, corresponding to a reliability index of 4.75. The 95% bootstrap interval for the failure probability was $[0,\ 5.0 \times 10^{-5}]$, and the corresponding interval for β was [3.89, 7.03]. These bounds reflect the fact that the lower tail is sparsely populated: the FE sample itself contains no failures relative to $\mathrm{LF} = 1.0$, so the reliability estimate still depends on the fitted lower tail of the peak load factor distribution and on the adopted model uncertainty factors.

The calibrated model reliability estimate should therefore be interpreted as a sample informed, model based structural reliability result. Its strength lies in the fact that the FE sample is generated from the calibrated nonlinear bridge model rather than from idealized resistance assumptions, and that the training sample meets a consistent *ultimate strain* criterion across all 200 realizations.

4. Discussion and Conclusions

This study presented a data-informed framework for structural reliability assessment of bridges by integrating measured dynamic behavior into structural model calibration. The main contribution of the paper is therefore methodological: OMA is not treated as an isolated identification exercise, but as the mechanism that constrains the support and

joint representation of the bridge before nonlinear safety assessment is carried out.

The updated support parameters are mechanically admissible and transferable to nonlinear analysis, and the calibrated nonlinear response indicates that the bridge is governed by support region hogging rather than by a purely midspan flexural mechanism. The repaired response sample further shows that the calibrated model can be traced consistently to the prescribed ultimate strain criterion across the full simulation set. The reported reliability should nevertheless be read as a model-based lower-tail estimate, because the FE sample itself contains no realizations below the failure threshold and the final probability of failure still depends on the fitted response distribution and the adopted JCSS model uncertainty factors. The main conclusions of the study are as follows.

(1) Operational modal analysis based on ambient vibration data provided sufficient information to identify the low order dynamic behavior of the bridge and to constrain the uncertain support and joint parameters that control the global response.
(2) A stagewise calibration strategy helped maintain parameter identifiability and produced a support representation that is both mechanically interpretable and transferable to nonlinear assessment.
(3) The nonlinear analyses indicate that safety assessment of this bridge is controlled by support-region behavior, showing that realistic support modeling is essential for credible resistance evaluation.
(4) The calibrated nonlinear response sample supports a high reliability level for the bridge, but the lower tail should still be interpreted through the adopted probabilistic model rather than as a directly observed empirical failure rate.

The central engineering implication is that reliability assessment of an existing bridge should be based on a model whose support behavior has first been calibrated against measured structural response.

Acknowledgments

The authors would like to acknowledge Project 101128171—NORISK—ERASMUS-EDU-2023-PEX-EMJM-MOB, funded by the European Union. Views and opinions expressed are those of the authors only and do not necessarily reflect those of the European Union or the European Education and Culture Executive Agency (EACEA). Neither the European Union nor the granting authority can be held responsible for them. This work was supported by FCT/MCTES under the R&D Unit Institute for Sustainability and Innovation in Structural Engineering (ISISE), under the references UID/4029/2025 (https://doi.org/10.54499/UID/04029/2025), UID/PRR/04029/2025 (https://doi.org/10.54499/UID/PRR/04029/2025) and UID/PRR2/04029/2025 (https://doi.org/10.54499/UID/PRR2/04029/2025), and under the Associate Laboratory Advanced Production and Intelligent Systems ARISE under reference LA/P/0112/2020 (https://doi.org/10.54499/LA/P/0112/2020). This work was also supported by national funds through FCT – Foundation for Science and Technology, from the Portuguese State Budget, under grant agreement PRT/BD/153494/2021 attributed to the third author, under the MIT Portugal Program.

References

Brownjohn, J. M. W., Filipe Magalhaes, Elsa Caetano, and Alvaro Cunha. 2010. "Ambient Vibration Re-Testing and Operational Modal Analysis of the Humber Bridge." *Engineering Structures* 32 (8): 2003–2018. https://doi.org/10.1016/j.engstruct.2010.02.034.

Cunha, Alvaro, Elsa Caetano, Filipe Magalhaes, Carlos Moutinho, and Antonio Campos Costa. 2012. "Finite Element Model Updating of a Bowstring-Arch Railway Bridge Based on Experimental Modal Parameters." *Engineering Structures* 40:413–435. https://doi.org/10.1016/j.engstruct.2012.03.013.

Dohler, Michael, Edwin Reynders, Filipe Magalhaes, Laurent Mevel, Guido De Roeck, and Alvaro Cunha. 2011. "Pre- and Post-Identification Merging for Multi-Setup OMA with Covariance-Driven SSI." In *Dynamics of Bridges, Volume 5,* 57–70. Springer. https://doi.org/10.1007/978-1-4419-9825-5_7.

Hester, D., K. Koo, Y. Xu, J. Brownjohn, and M. Bocian. 2019. "Boundary Condition Focused Finite Element Model Updating for Bridges." *Engineering Structures* 198:109514. https://doi.org/10.1016/j.engstruct.2019.109514.

Huang, M., H. Zhu, L. Li, and W. Guo. 2008. "Dynamic Test and Finite Element Model Updating of Bridge Structures Based on Ambient Vibration." *Frontiers of Structural and Civil Engineering* 2 (2): 139–144. https://doi.org/10.1007/s11709-008-0028-4.

Jaishi, Bishnu, and Wei-Xin Ren. 2007. "Finite Element Model Updating Based on Eigenvalue and Strain Energy Residuals Using Multiobjective Optimisation Technique." *Mechanical Systems and Signal Processing* 21 (5): 2295–2317. https://doi.org/10.1016/j.ymssp.2006.09.008.

Joint Committee on Structural Safety. 2023. *JCSS Probabilistic Model Code: Model Uncertainties.* Online resource, Accessed 2026-03-25.

Kamariotis, Athanasios, Eleni Chatzi, and Daniel Straub. 2023. "A Framework for Risk-Informed Structural Health Monitoring of Bridges Under Environmental and Operational Variability." *Structural Health Monitoring* 22 (2): 1105–1128. https://doi.org/10.1177/14759217221113862.

———. 2022. "Value of Information from Vibration-Based Structural Health Monitoring Extracted via Bayesian Model Updating." *Mechanical Systems and Signal Processing* 166:108465. https://doi.org/10.1016/j.ymssp.2021.108465.

Magalhaes, Filipe, Alvaro Cunha, and Elsa Caetano. 2009. "Online Automatic Identification of the Modal Parameters of a Long Span Arch Bridge." *Mechanical Systems and Signal Processing* 23 (2): 316–329. https://doi.org/10.1016/j.ymssp.2008.05.003.

Malveiro, Joel, Diogo Ribeiro, Carlos Sousa, and Rui Calcada. 2018. "Model Updating of a Dynamic Model of a Composite Steel-Concrete Railway Viaduct Based on Experimental Tests." *Engineering Structures* 164:40–52. https://doi.org/10.1016/j.engstruct.2018.02.057.

McKay, M. D., R. J. Beckman, and W. J. Conover. 1979. "A Comparison of Three Methods for Selecting Values of Input Variables in the Analysis of Output from a Computer Code." *Technometrics* 21 (2): 239–245. https://doi.org/10.1080/00401706.1979.10489755.

McKenna, Frank. 2011. "OpenSees: A Framework for Earthquake Engineering Simulation." *Computing in Science & Engineering* 13 (4): 58–66. https://doi.org/10.1109/MCSE.2011.66.

McKenna, Frank, Michael H. Scott, and Gregory L. Fenves. 2010. "Nonlinear Finite-Element Analysis Software Architecture Using Object Composition." *Journal of Computing in Civil Engineering* 24 (1): 95–107. https://doi.org/10.1061/(ASCE)CP.1943-5487.0000002.

Melchers, Robert E., and Andre T. Beck. 2017. *Structural Reliability Analysis and Prediction.* 3rd ed. John Wiley & Sons. ISBN: 9781119265993.

OpenSees Documentation. 2026. *ASDConcrete1D Material.* Online material model documentation, Accessed 2026-03-26.

Pasca, Dag P., and Diego Federico Margoni. 2025. "pyOMA2: A Python module for conducting operational modal analysis." *Journal of Open Source Software* 10 (115): 7656. https://doi.org/10.21105/joss.07656.

Pasca, Pietro, Alberto Sestieri, and Walter D'Ambrogio. 2022. "PyOMA and PyOMA_GUI: Operational Modal Analysis Made Easy." *SoftwareX* 20:101216. https://doi.org/10.1016/j.softx.2022.101216.

Peeters, Bart, and Guido De Roeck. 2001. "Stochastic System Identification for Operational Modal Analysis: A Review." *Journal of Dynamic Systems, Measurement, and Control* 123 (4): 659–667. https://doi.org/10.1115/1.1410370.

Reynders, Edwin, Johan Houbrechts, and Guido De Roeck. 2012a. "Fully Automated (Operational) Modal Analysis." *Mechanical Systems and Signal Processing* 29:228–250. https://doi.org/10.1016/j.ymssp.2012.01.007.

Reynders, Edwin J., Johan Houbrechts, and Guido De Roeck. 2012b. "System Identification Methods for (Operational) Modal Analysis: Review and Comparison." *Archives of Computational Methods in Engineering* 19 (1): 51–124. https://doi.org/10.1007/s11831-012-9069-x.